AIAA Paper No. 69-877

STABILITY ANALYSIS OF APOLLO-SATURN V PROPULSION AND STRUCTURE FEEDBACK LOOP

by

GEORGE L. von PRAGENAU
NASA Marshall Space Flight Center
Huntsville, Alabama

AIAA Guidance, Control, and Flight Mechanics Conference

PRINCETON, NEW JERSEY/AUGUST 18-20, 1969

STABILITY ANALYSIS OF APOLLO-SATURN V PROPULSION AND STRUCTURE FEEDBACK LOOP

by

George L. von Pragenau*
NASA, George C. Marshall Space Flight Center
Marshall Space Flight Center, Alabama 35812

Abstract

The propulsion and the structure of a space vehicle form a feedback loop through inertial coupling referred to as the pogo phenomenon and experienced with the Thor, Titan, and Apollo-Saturn V space vehicles. Fortunately, the pogo oscillations reached a limit cycle before becoming destructive. However, in some cases, vibrations were high enough to become intolerable to astronauts or to cause undue acceleration loads on space vehicle components. Therefore, great efforts were made to analyze the stability situation and to eliminate pogo oscillations of the Apollo-Saturn V space vehicles. Several aerospace companies cooperated with the Marshall Space Flight Center in solving the problem for the first moon flight of the Apollo-Saturn 503 and subsequent launchings.

This paper treats the multiforce feedback, first experienced in the Saturn V space vehicle, from the general viewpoint of multivariable feedback systems and demonstrates the application of the Nyquist plot. Pogo loop components, such as the propulsion system and especially the eigenvalue problem of the structural model, are discussed. A comparison is made between the linearly unstable first flight stage of the AS-502 vehicle and one of the later vehicles, the AS-504, which was successfully stabilized by the addition of a helium gas accumulator to cushion the propellant.

Introduction

Self-induced longitudinal oscillations were experienced within the past ten years on practically all large liquid propellant rockets: the Atlas, Thor, Titan, and finally the Saturn V. The rockets usually oscillated with their ends moving against each other, like a youngster does on a pogo stick. The comparison led to the term "pogo effect" which can be interpreted as propulsion-generated oscillations. This classification may be too inclusive because it covers several phenomena which have different causes. Falling in this category are, for example, the pressure regulator feedback on the Atlas and the propulsion to structure feedback on the Thor, Titan, first stage of the Saturn V, and more recently a so-called mini pogo on the second stage of the Saturn V involving only the center engine area.

The pogo phenomenon found wide attention and was treated by several authors in publications and reports peaking around 1965.[1-6]

The coincidence of the first longitudinal vehicle mode and the first propellant line mode was considered as the main cause of the pogo phenomenon. The possibility of the coincidence with line modes for higher resonances was explored, but the resonance amplification appeared to be negligible. Now, this assumption about the higher frequencies (10 to 30 Hz) has changed, and it is generally agreed that these frequencies deserve a careful analysis. Modeling of the structure, tanks, and propellant feed lines led finally to the inclusion of 30 resonances. There is approximately one resonance per 1 Hz frequency increment, in contrast to other cases, such as the attitude control systems, which usually have only a few significant resonances.

The analysis demonstrated permits a survey of the stability status in a wide frequency range, but is restricted to a linear and time invariant model which cannot reproduce the limit cycle effect observed in flight. Most likely, the limit cycle was caused by a tuning/detuning of time variable resonances (predominant on the first flight stage, S-IC), a nonlinear loop gain which decreases at higher amplitudes (well pronounced on the second stage, S-II), or possibly both. In most cases, the pogo oscillations had a football-shaped envelope, building up slowly like a slightly unstable linear system before damping out.

During the analysis of the Saturn V pogo effect, it became clear that the inboard and the outboard rocket motors moved very independently because of sufficient structural flexibility in the thrust frame. The multiforce feedback required multivariable loop analysis instead of the single loop approach. This condition was contrary to the pogo effects of earlier vehicles and the attitude control case in which only one feedback force had to be considered. The pogo oscillations were finally eliminated for the first flight stage of the Saturn V vehicles beginning with the first moon flight, the AS-503.[7] Stability was attained by placing a helium accumulator near the lox pump inlets where it attenuated propellant pressure oscillations.

---

*Senior Aerospace Engineer, Research and Development Analysis Office, Astrionics Laboratory

The detailed discussion in this paper of the pogo phenomenon is initiated with a simple model to illustrate important pogo loop components. The following sections present the propulsion system equations, the eigenvalue model of the structure, and finally the pogo loop in a matrix form including the stability analysis of multivariable systems. The stability of such complex systems is proven by a single Nyquist plot.

Simplified Pogo Phenomenon*

Before plunging into the complexity of the problem, it is very instructive to study the simple model shown in Figure 1. This model has all the essential ingredients of the pogo phenomenon: propellant mass, cavitation stiffness at the propellant pump inlet, orifice effect of pump inlet, vehicle mass, and the thrust's sensitivity to propellant pressure at the pump's inlet.

The pogo loop can best be described through the involved components, starting with a small thrust change T which forces the vehicle and propellant masses to accelerate. The accelerated propellant mass, here the liquid oxygen in the tank, exerts a pressure force onto the cavitation stiffness K_s which transmits it to the pump's inlet. This pressure affects the propellant's flow which feeds the combustion in the rocket motor; thus the thrust is changed by this pressure. Then the whole process starts again in a feedback fashion.

The propulsion system's sensitivity is simply described by a constant gain E with P_s, the propellant force, and T, the thrust. Actually all variables represent small variations about a quiescent point. Also introduced are an external disturbance force f at the thrust point and the force F_s which accelerates the vehicle. The equations are

$$P_s \cdot E = T \tag{1}$$

$$F_s = P_s \cdot E + f \tag{2}$$

The structural model, which includes the propellant, cavitation, and orifice effect, relates the propellant force P_s to force F (all equations are given in Laplace transform):

$$P_s = \frac{F_s}{1 + \frac{m}{m_s} + s\frac{m}{D_s} + s^2\frac{m}{K_s}} \tag{3}$$

The closed loop equation results from equations (2) and (3):

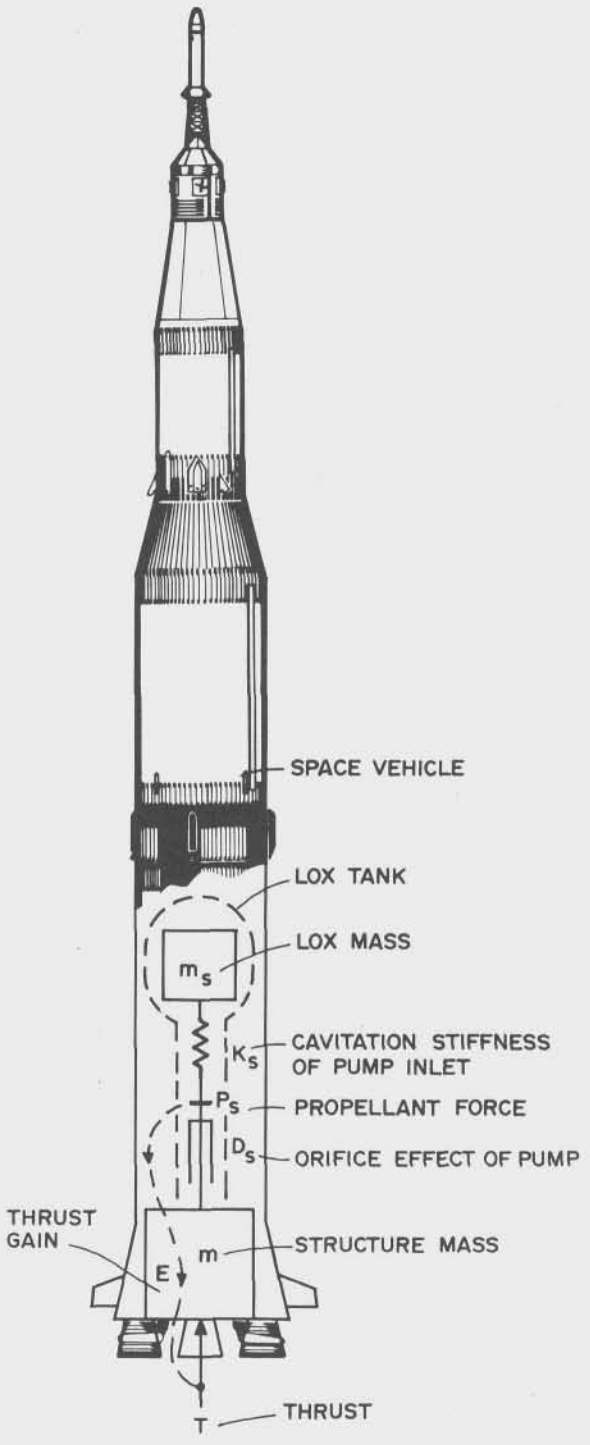

FIGURE 1. SIMPLIFIED POGO LOOP MODEL

$$P_s = \frac{f}{1 + \frac{m}{m_s} - E + s\frac{m}{D_s} + s^2\frac{m}{K_s}} \tag{4}$$

Equation (4) gives the response of the propellant force P_s to a disturbance f. The thrust response

*The nomenclature is listed on pages 13 and 14.

can be obtained by substituting equation (4) into equation (1); however, this is of no consequence for the stability analysis because the gain E is assumed constant.

The zeros in the denominator of equation (4) indicate whether the system is stable or unstable. Stability requires that the roots have negative real parts which can easily be determined in this simple second order system. It results that the constant $1+\frac{m}{m_s} - E$ must be positive for stability; i.e., gain E is limited by the stability criterion

$$E < 1 + \frac{m}{m_s} \qquad (5)$$

The engine's gain should not be too high; in fact, it should be less than one if the mass ratio of vehicle structure to liquid oxygen is assumed to be negligible. All Saturn V vehicles have an E gain above one, leading to a potential "pogo" stability problem. However, it must be emphasized that this analysis, which is overly simplified, is given for illustration purposes only. One of the simplifications is that the total propellant mass is at the pump inlet, while in reality only a small mass portion presses against the inlet. Another simplification is that the vehicle is only one mass instead of a resonant body with many resonances. A reduction of the gain E below one would be ideal, but for practical reasons other means are used to make the system stable[7] (see the He accumulator on Fig. 2).

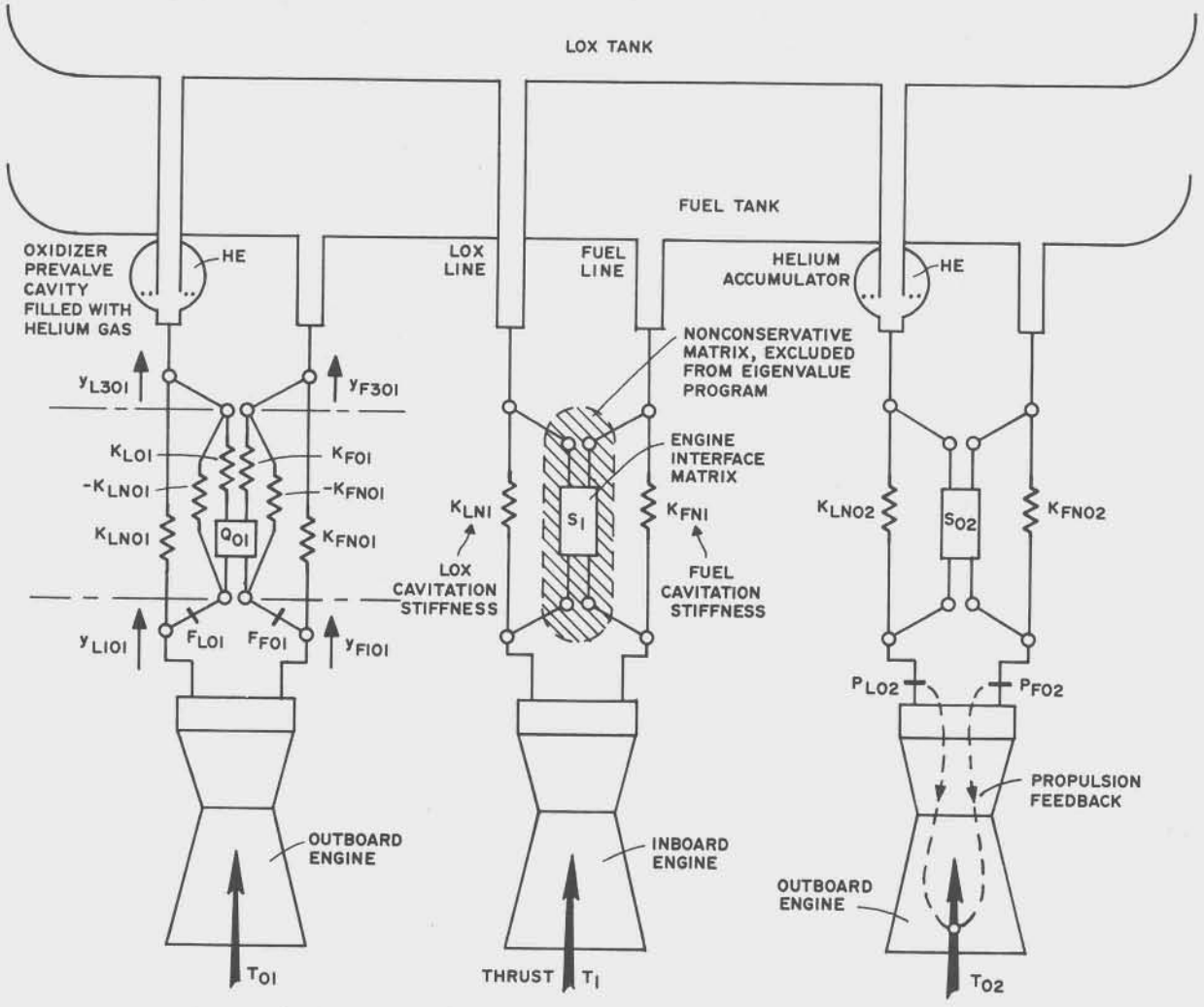

FIGURE 2. INTERFACE OF PROPULSION & VEHICLE STRUCTURE
(Cross-Bar on Line, +, Indicates Pressure Force)

Propulsion System

The essential elements of the propulsion system are the centrifugal pumps, the engine's combustion process, and the cavitation forming at the pump's intake. The centrifugal pumps feed the rocket engines with propellants such as liquid oxygen for oxidizer and kerosene or liquid hydrogen for fuel and contribute most of the dynamic behavior involved in pogo oscillations. The dynamic behavior of the engine's combustion process is far above the frequency range; therefore, it is practically a constant gain figure. Both of these effects are described by engine transfer functions with the propellant pressure forces at the pump inlets as inputs and the propellant flows and the thrust as outputs (Table 1).[8] The cavitation forming at the pump's intake produces a cushioning effect for the propellant in the feed lines, and greatly influences the propellant's resonances. Formation of the cavitation depends on temperature, pressure, and velocity differences between the intake flow and the pump speed.

Because of great difficulties in the dynamic analysis of the propulsion system, it was necessary to find the engine transfer function and the so-called cavitation stiffness[4] through pump flow tests and captive engine firings. It was also necessary to restrict the modeling to the linearized type because of the difficulties in obtaining nonlinear models.

The interface variables of the pogo loop are depicted in Figure 2 and with more detail in Figures 3 and 4. The propellant flow is proportional to velocity and, consequently, to propellant displacement (Figs. 3 and 4). The pump inlet acts like an orifice with some cross coupling between the fuel and the lox side as expressed by the vector equation

$$(P_L\ P_F)\ \frac{1}{s}\begin{pmatrix} q_{LL} & q_{LF} \\ q_{FL} & q_{FF} \end{pmatrix} = (y_{L1}-y_{L2},\ y_{F1}-y_{F2}) \quad . (6)$$

All variables are actually small variations about an equilibrium point and the coefficients result from linear approximation.

TABLE 1. F-1 ENGINE TRANSFER FUNCTION

$\frac{\partial V_L}{\partial P_L} = q_{LL}\left[\frac{m}{Ns}\right]$	$\frac{0.94 \cdot 10^{-5}(1 + s0.67 \cdot 10^{-1})}{(1 + s0.153)\ (1 + s0.229 \cdot 10^{-2})}$
$\frac{\partial V_F}{\partial P_L} = q_{LF}\left[\frac{m}{Ns}\right]$	$\frac{0.225 \cdot 10^{-5}\ (1 - s0.533 \cdot 10^{-1})}{(1 + s0.164)\ (1 + s0.69 \cdot 10^{-2})\ (1 + s0.307 \cdot 10^{-2} + s^2 0.62 \cdot 10^{-5})}$
$\frac{\partial V_L}{\partial P_F} = q_{FL}\left[\frac{m}{Ns}\right]$	$\frac{-0.307 \cdot 10^{-5}\ (1 + s0.514 \cdot 10^{-1})\ (1 - s0.355 \cdot 10^{-2})}{(1 + s0.172)\ (1 + s0.132 \cdot 10^{-1})}$
$\frac{\partial V_F}{\partial P_F} = q_{FF}\left[\frac{m}{Ns}\right]$	$\frac{0.126 \cdot 10^{-5}\ (1 + s0.45)\ (1 + s0.144 \cdot 10^{-1})}{(1 + s0.22)\ (1 + s0.165 \cdot 10^{-1})\ (1 + s0.356 \cdot 10^{-2})}$
$\frac{\partial T}{\partial P_L} = g_L\left[\frac{N}{N}\right]$	$\frac{5.55\ (1 + s0.512 \cdot 10^{-1})}{(1 + s0.16)\ (1 + s0.226 \cdot 10^{-2})}$
$\frac{\partial T}{\partial P_F} = g_F\left[\frac{N}{N}\right]$	$\frac{-1.12\ (1 - s0.857 \cdot 10^{-1})\ (1 + s0.388 \cdot 10^{-2})}{(1 + s0.168)\ (1 + s0.288 \cdot 10^{-2})\ (1 + s0.222 \cdot 10^{-2})}$

Equation (6) relates the lox and fuel forces P_L and P_F to the relative displacements $y_{L1} - y_{L2}$ and $y_{F1} - y_{F2}$ of the lox and fuel propellant. The engine flow matrix is defined by Q which is equivalent to the reciprocal dashpot D_s^{-1} shown in Figure 1:

$$\frac{1}{s}\begin{pmatrix} q_{LL} & q_{LF} \\ q_{FL} & q_{FF} \end{pmatrix} = Q \quad . \quad (7)$$

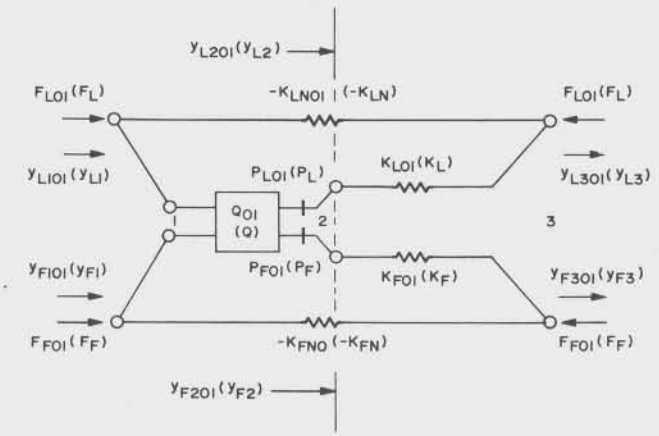

FIGURE 3. ENGINE INTERFACE MATRIX S_{01}; S_I AND S_{02} ARE SIMILAR. (The negative stiffness cancels the stiffness of the structural model.)

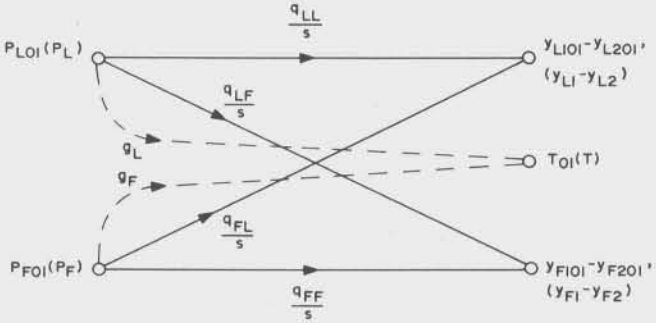

FIGURE 4. ENGINE FLOW MATRIX Q (⟶) AND ENGINE THRUST (⇢) FLOW DIAGRAMS

The components of Q are given in Table 1. The propellant forces P_L and P_F are directly related to the rocket engine's thrust by the relation

$$\begin{pmatrix} P_L & P_F \end{pmatrix} \begin{pmatrix} g_L \\ g_F \end{pmatrix} = T \quad . \tag{8}$$

The thrust gain is defined by a column vector which is similar to the gain E of equation (1):

$$\begin{pmatrix} g_L \\ g_F \end{pmatrix} = G \quad . \tag{9}$$

The components of G result from the pump flow characteristics and from the engine's combustion (Table 1). All variables are given as row vectors because this form corresponds well with flow diagrams.

The flow matrix Q describes the orifice-like effect of the lox and the fuel pump inlets for one engine; the springs K_L and K_F represent the cavitation at the pump inlets for the lox or the fuel side, respectively (Fig. 3).

The propellant feed lines are terminated by the cavitation effect in series with the orifice effect of the pumps. It is practical at first to neglect the orifice effect and to terminate the feed lines with the cavitation stiffness only (K_{LN} for the lox side and K_{FN} for the fuel side). This permits the use of an energy-conserving system from the vehicle's structure down to the engine pump inlets. The resonances are then more realistic than the resonances of open-ended line models which are another possibility to model the structure; however, the terminated line case helps the interpretation and gives a better selection of significant structural resonances.

A comparison of Figures 2 and 3 shows that the cavitation stiffnesses K_{LN} and K_{FN} of the structural model (Fig. 2) are parallel to the negative stiffnesses $-K_{LN}$ and $-K_{FN}$ (Fig. 3) of the engine model. This permits an exchange of components when joining the structural model with the engine model. It actually replaces the cavitation stiffnesses K_{LN} and K_{FN} by a series arrangement of the cavitation stiffnesses K_L and K_F with the pump orifice effect. Thus the actual system is restored when the energy-conserving structural model is connected with the engine model.

The relative displacements $y_{L2} - y_{L3}$ and $y_{F2} - y_{F3}$ shown in Figure 3 are related through the cavitation stiffness to the propellant forces P_L and P_F for the lox L and the fuel side F, respectively:

$$(P_L\ P_F) \begin{pmatrix} \frac{1}{K_L} & 0 \\ 0 & \frac{1}{K_F} \end{pmatrix} = (y_{L2}-y_{L3}, y_{F2}-y_{F3}) \quad . \tag{10}$$

The cavitation matrices are defined by

$$K = \begin{pmatrix} K_L & 0 \\ 0 & K_F \end{pmatrix} \text{and } K_N = \begin{pmatrix} K_{LN} & 0 \\ 0 & K_{FN} \end{pmatrix} . \tag{11}$$

The external forces F_L and F_F (Fig. 3) act on the structural model (Fig. 2) and are formed after adding the effect of the negative stiffnesses $-K_{LN}$ and $-K_{FN}$:

$$(P_L\ P_F) + (y_{L1}-y_{L3}, y_{F1}-y_{F3}) \begin{pmatrix} -K_{LN} & 0 \\ 0 & -K_{FN} \end{pmatrix} =$$

$$= (F_L\ F_F) \tag{12}$$

The relative deflections $y_{L1}-y_{L3}$ and $y_{F1}-y_{F3}$ are directly related to the propellant forces P_L and P_F after adding equations (6) and (10):

$$(P_L P_F)(Q+K^{-1}) = (y_{L1}-y_{L3}, y_{F1}-y_{F3}) \quad . \quad (13)$$

Equation (13) is now substituted into equation (12):

$$(P_L P_F)[I-(Q+K^{-1})K_N] = (F_L F_F) \quad (14)$$

The matrix of this equation is defined by

$$C = I - (Q + K^{-1})\ K_N \quad (15)$$

The rigid connection of the outboard engine allows all outboard engines to be treated as one large engine; therefore, the indices 01 and 02 are interchanged with the index 0. Similarly, the pump inlets on the lox and fuel side practically move together. Consequently, the indices become $L10 = F10 = 0$ and $L1I = F1I = I$. Another index simplification is introduced for point 3 (Fig. 3) where we now have $L30 = L0$, $F30 = F0$, $L3I = LI$, and $F3I = FI$.

The relative deflections are expressed in forms of the new indices:

$$y_{L10} - y_{L30} = y_0 - y_{L0} = -\Delta y_{L0} \quad (16)$$

$$y_{F10} - y_{F30} = y_0 - y_{F0} = -\Delta y_{F0}$$

$$y_{L1I} - y_{L3I} = y_I - y_{LI} = -\Delta y_{LI}$$

$$y_{F1I} - y_{F3I} = y_I - y_{FI} = -\Delta y_{FI}$$

All forces that act on the structure are now arranged in a vector form by inserting definitions (9) and (15) into a partitioned matrix [see also equations (8) and (14)]:

$$(P_{L0} P_{F0} P_{LI} P_{FI}) \begin{pmatrix} C_0 & G_0 & 0\,0 & 0 \\ 0\,0 & 0 & C_I & G_I \end{pmatrix} = (F_{L0} F_{F0} T_0 F_{LI} F_{FI} T_I) \quad (17)$$

If all engines are equal, then $C_0 = C_I$ and $G_0 = G_I$.

Equation (13) relates the force vector $(P_L P_F)$ to the relative displacements of definition (16). This is also expressed in a partitioned matrix form:

$$(P_{L0} P_{F0} P_{LI} P_{FI}) \begin{pmatrix} Q_0 + K_0^{-1} & 0\ 0 & 0 \\ 0\ 0 & 0 & Q_I + K_I^{-1} \end{pmatrix} = = -(\Delta y_{L0} \Delta y_{F0} \Delta y_{LI} \Delta y_{FI}) \quad . \quad (18)$$

If all engines are equal, then $Q_0 + K_0^{-1} \doteq (Q + K^{-1})/4$ for four outboard engines.

Vehicle Structure Dynamic

The elastodynamic behavior of the space vehicle is given by discrete masses and springs which describe the inertia and elastic behavior of the structure, tanks, lines, and liquid propellants.[9]

The coupling of lateral motions into the longitudinal direction was assumed to be small because of the vehicle's symmetry; therefore only the longitudinal response is considered here for the pogo loop analysis.

The displacement of each free mass movement is taken as a component of a displacement vector y (row vector). Similarly we define a force vector F whose components are forces on each free mass. Further we denote a mass matrix M and a stiffness matrix K_e. Thus the following vector equation is obtained in Laplace transform for the system initially at zero-rest (initially without displacement or velocity):

$$y(s^2 M + K_e) = F \quad (19)$$

Equation (19) relates the displacement vector y to the vector F.

The degrees of freedom are often too high (up to hundreds) to permit a direct use of this equation; therefore, an eigenvalue analysis is employed to find significant resonances which are then used to reduce the degrees of freedom.

A linear transformation $y = z \cdot U$, a postmultiplication of equation (19) by U', and a square root factorization of the mass matrix M yield

$$zUM^{\frac{1}{2}} (s^2 I + M^{-\frac{1}{2}} K_e M^{-\frac{1}{2}}) M^{\frac{1}{2}} U' = FU' \quad , \quad (20)$$

where $UM^{\frac{1}{2}}$ is considered as the eigenvector matrix of the symmetric matrix $M^{-\frac{1}{2}} K_e M^{-\frac{1}{2}}$. Its eigenvalues s^2 are real because of the symmetry and are distinct because a mechanical structure is represented. The latter ensures that the eigenvectors (rows of $UM^{\frac{1}{2}}$) are orthogonal to each other.[10,11] The orthogonality helps to invert the matrix on the left of equation (20) by

forming the diagonal matrices UMU' and UKU' which are denoted as the generalized mass matrix and the generalized stiffness matrix, respectively.

The determination of the eigenvector matrix $UM^{\frac{1}{2}}$ from the matrix $M^{-\frac{1}{2}} K_e M^{-\frac{1}{2}}$ yields the matrix U. Equation (20) is diagonalized by the mode shape matrix U:

$$z\,(s^2 UMU' + UK_e U') = FU' \tag{21}$$

Equation (21) is easily inverted and then changed to an equation explicit in y:

$$y = FU'\,(s^2\,UMU' + UK_e U')^{-1} U \tag{22}$$

Note that the generalized mass matrix UMU' depends on free scale factors of the eigenvectors of $UM^{\frac{1}{2}}$ which, for example, could make UMU' a unit matrix. Often, however, it is preferred to normalize the mode shape vectors of matrix U. The inverted matrix of equation (22) appears as follows:

$$(s^2 UMU' + UK_e U')^{-1} =$$

$$= \begin{pmatrix} \frac{1}{s^2 m_1} & 0 & 0 & \cdot\cdot \\ 0 & \frac{1}{(s^2+\omega_2^2)\,m_2} & 0 & \cdot\cdot \\ 0 & 0 & \frac{}{(s^2+\omega_3^2)\,m_3} & \cdot\cdot \\ \cdot & \cdot & \cdot & \cdot\cdot \end{pmatrix}. \tag{23}$$

Observe that the resonances are the poles at $s = \pm j\omega_i$, $i = 2, 3 \ldots$.

The small damping of the vehicle is simply introduced by adding damping to each second order polynomial. Equation (23) is now augmented and redefined:

$$\Omega^{-1} = \begin{pmatrix} \frac{1}{s^2 m_1} & 0 & 0 & \cdot \\ 0 & \frac{1}{(s^2+s2\zeta_2\omega_2+\omega_2^2)\,m_2} & 0 & \cdot \\ 0 & 0 & \frac{1}{(s_2+s2\zeta_2\omega_3+\omega_3^2)\,m_3} & \cdot \\ \cdot & \cdot & \cdot & \cdot \end{pmatrix}. \tag{24}$$

This matrix replaces matrix (23) and is used for the structural model equation

$$y = FU'\Omega^{-1}U \tag{25}$$

Pogo Loop System

Equations (17) and (18) represent the propulsion system, and equation (25) represents the vehicle structure. A substitution within those equations results in the pogo loop equation, but first the mode shape matrices U' and U, equation (25), are described in more detail.

Equation (18) needs only four mode shape components; therefore, the mode shape matrix U is reduced to the following form:

$$U = -(\Delta Y_{L0} \Delta Y_{F0} \Delta Y_{LI} \Delta Y_{FI}) \tag{26}$$

Equation (17) has only six forces on its right side; therefore, the mode shape matrix U' is reduced to the six terms which multiply with the six force components:

$$U' = \begin{pmatrix} \Delta Y'_{L0} \\ \Delta Y'_{F0} \\ Y'_0 \\ \Delta Y'_{LI} \\ \Delta Y'_{FI} \\ Y'_I \end{pmatrix} \tag{27}$$

All components of this matrix are row vectors which have themselves for each resonance frequency one component. The components of the U matrix are the same except they are transposed, making them column vectors.

The pogo loop equation is obtained by substituting equation (17) into equation (25) and then equating the result with equation (18). Besides manipulating the equations, it is helpful to introduce external disturbance forces (D_0, D_I) at the outboard and the inboard engine group to define an input-output relation:

$$-(P_{L0}P_{F0}P_{LI}P_{FI})\begin{pmatrix} Q_0 + K_0^{-1} & \begin{matrix}0 & 0\\0 & 0\end{matrix} \\ \begin{matrix}0 & 0\\0 & 0\end{matrix} & Q_I + K_I^{-1}\end{pmatrix} =$$

$$= (P_{L0}P_{F0}P_{LI}P_{FI})\begin{pmatrix} C_0 & G_0 & \begin{matrix}0&0&0\\0&0&0\end{matrix} \\ \begin{matrix}0&0&0\\0&0&0\end{matrix} & C_I & G_I\end{pmatrix}\begin{pmatrix}\Delta Y'_{L0}\\ \Delta Y'_{F0}\\ Y'_0\\ \Delta Y'_{LI}\\ \Delta Y'_{FI}\\ Y'_I\end{pmatrix} \Omega^{-1}\ (\Delta Y_{L0}\Delta Y_{F0}\Delta Y_{LI}\Delta Y_{FI}) + \tag{28}$$

$$+ (D_0 D_I)\begin{pmatrix}Y'_0\\ Y'_I\end{pmatrix}\ \Omega^{-1}\ (\Delta Y_{L0}\Delta Y_{F0}\Delta Y_{LI}\Delta Y_{FI})$$

or

$$(P_{L0}P_{F0}P_{LI}P_{FI})\left[\begin{pmatrix} Q_0 + K_0^{-1} & \begin{matrix}0 & 0\\0 & 0\end{matrix} \\ \begin{matrix}0 & 0\\0 & 0\end{matrix} & Q_I + K_I^{-1}\end{pmatrix} + \begin{pmatrix} C_0 & G_0 & \begin{matrix}0&0&0\\0&0&0\end{matrix} \\ \begin{matrix}0&0&0\\0&0&0\end{matrix} & C_I & G_I\end{pmatrix}\begin{pmatrix}\Delta Y'_{L0}\\ \Delta Y'_{F0}\\ Y'_0\\ \Delta Y'_{LI}\\ \Delta Y'_{FI}\\ Y'_I\end{pmatrix} \Omega^{-1}\ (\Delta Y_{L0}\Delta Y_{F0}\Delta Y_{LI}\Delta Y_{FI})\right] = \tag{29}$$

$$= -(D_0 D_I)\begin{pmatrix}Y'_0\\ Y'_I\end{pmatrix}\ \Omega^{-1}\ (\Delta Y_{L0}\Delta Y_{F0}\Delta Y_{LI}\Delta Y_{FI}).$$

This equation represents the pogo loop as it is given in Figure 5.

Pogo Loop Stability

The pogo loop is a case of multivariable feedback in which the feedback variable is not a scalar but a vector. The feedback is given by a matrix with plenty of cross-coupling as shown in Figure 5. The elements of the matrix are transfer functions which are more complicated than the single s operator in the diagonal elements of a state transition matrix.[11,12] However, because the matrix of equation (29) is considerably smaller than that in the state space approach, equation (29) is more suitable for a stability analysis.

The linearity and the time invariance of the model permitted the inclusion of many resonances which are relatively dense in the pogo case. The approach appears to be well justified to predict stability because the unstable buildup of actual pogo oscillations resemble oscillations of slightly unstable linear systems and because the vehicle resonances change relatively slow during flight. The nonlinearities are assumed monotonic without any abrupt changes as in the case of bang-bang control systems.

The understanding of matrix feedback stability has improved in recent years as reflected in the literature.[13,14,15] Erroneous criteria were abandoned and the approaches seem to have become simpler. The method used here follows the criteria presented by other authors,[14,15] but selects the special case where the matrices have only stable elements. This approach permits great simplifications for the proof and the application. Generally, the method becomes remotely comparable to a state space type of stability analysis if the Laplace transformed matrix sI is replaced by a matrix with stable transfer function elements.

Lack of knowledge in treating matrix feedback cases has often led to simplification which caused doubt about the validity of the analysis. For example, Nyquist plots are sometimes obtained by opening one loop only while other loops remain closed. The interpretation of the stability margins then becomes obscured, mainly because of the unpredictable influence of the closed loops in the "open loop system." The stability status of the closed loops must then be analyzed by additional Nyquist plots or root finding routines, thus producing several stability margins which cannot be combined or expressed by a single term. Variation of parameters can help to find the stability limit, but this method still does not preclude a possible pole-zero cancellation if only the open loop plot is evaluated.

The method presented here treats the problem from the closed loop standpoint. Equation (29) is now simplified by using the following matrix and vector definitions:

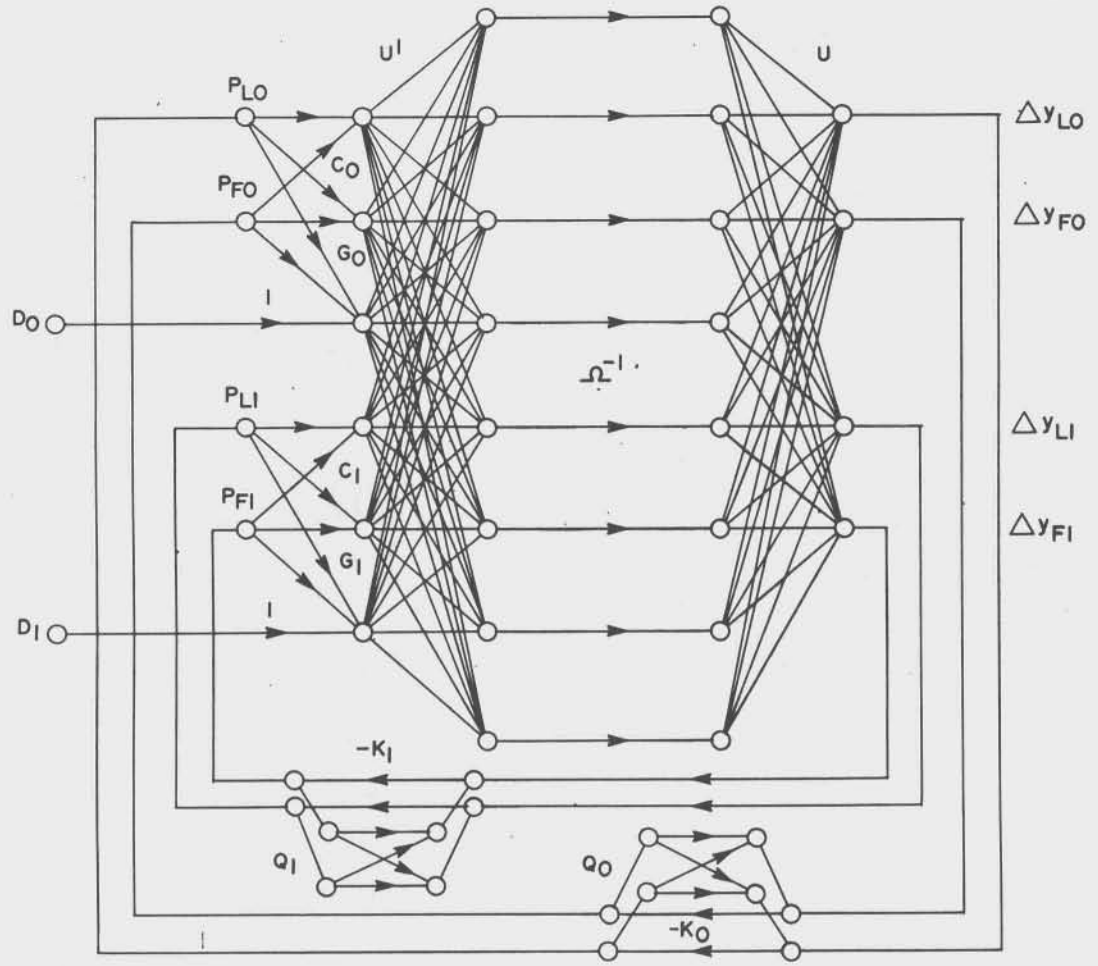

FIGURE 5. POGO LOOP FLOW DIAGRAM

$$A = \begin{pmatrix} Q_0 + K_0^{-1} & 0 & 0 \\ 0 & 0 & Q_I + K_I^{-1} \end{pmatrix} + \begin{pmatrix} C_0 & G_0 & 0 & 0 & 0 \\ 0 & 0 & 0 & C_I & G_I \end{pmatrix} \begin{pmatrix} \Delta Y'_{L0} \\ \Delta Y'_{F0} \\ Y'_0 \\ \Delta Y'_{LI} \\ \Delta Y'_{FI} \\ Y'_I \end{pmatrix} \Omega^{-1} (\Delta Y_{L0} \Delta Y_{F0} \Delta Y_{LI} \Delta Y_{FI}) \quad . \tag{30}$$

$$B = -\begin{pmatrix} Y'_0 \\ Y'_I \end{pmatrix} \Omega^{-1} (\Delta Y_{L0} \Delta Y_{F0} \Delta Y_{LI} \Delta Y_{FI}) \quad . \tag{31}$$

$$P = (P_{L0} P_{F0} P_{LI} P_{FI}) \tag{32}$$

$$D = (D_0 D_I) \tag{33}$$

Equation (29) now changes to

$$P \cdot A = D \cdot B \tag{34}$$

This equation is typical of any linear and time invariant feedback case in which we relate disturbance D to the loop variable P. A matrix inversion expresses P explicitly:

$$P = D \cdot B \cdot \text{adj}\,(A) / |A| \tag{35}$$

The loop variables behave stably if the elements of the matrix $B \cdot \text{adj}(A)/|A|$ are stable. This is certainly true if we can show that each element of the matrix $B \cdot \text{adj}(A)/|A|$ has a Nyquist plot[16,17] about the origin which indicates stability. This definitely is not an open loop concept but checks stability without loosing sight of all poles and zeros of the system.

The system is assumed to be "observable and controllable" because all involved elements of the pogo loop are retained in the closed loop approach and no pole-zero cancellations occurred.

This stability criterion is necessary and sufficient for the input/output relation between a disturbance and the feedback vector variable. However, the method needs too many plots; e.g., one for each element of the matrix, not to mention that the zeros of the elements must also be known (encirclements = no. of zeros - no. of poles).

One plot would be more convenient, preferably from the determinant $|A|$ [equation (35)]. Then, however, we must avoid any pole-zero cancellations within the determinant and must check for possibly unstable poles of the classical adjoint of A.[15] The poles of the matrix B must also be checked, but this is a separate stability problem. All these problems are eliminated when unstable poles in the elements of the matrices adj (A) and B are avoided. The statement can be reduced to the requirement that only matrices A and B must be stable since the poles of the adjoint of matrix A are at most identical to the poles of matrix A.

The state space approach demonstrates how unstable poles can be avoided when formulating the problem. Matrix A becomes $A = sI - H$, where H is the constant matrix of the state vector equation $\dot{y} = yH + u$.[11,12] Matrix A assumes, in this case, its maximally possible size, but for linear and time invariant cases the system can be described by a much smaller matrix A whose elements are complicated transfer functions. As long as these elements are stable, they are admitted. The object is to keep matrix A as small as possible.

The stability of the elements of matrices A and B [equations (30) and (31)] follows from the stability of their building blocks: matrices Q, K, C, G, and Ω^{-1} [Table 1, and definitions (7), (9), (11), (15), and (24)]. These building blocks are connected with addition, matrix multiplications, and insertion in matrix partitions. Therefore, the poles of the final matrix elements are the poles of the building blocks which apparently have only stable poles.

Now a Nyquist plot about the origin from the determinant $|A|$ is computed.* The number of the clockwise encirclements equals the number of unstable zeros of $|A|$.

Two examples are given for first flight stages of the Saturn V vehicle at 120 seconds of flight time: the AS-502 which is linearly unstable at 5 Hz and the AS-504 which is stabilized by a helium accumulator at the lox pump inlets (Figs. 6 and 7). The "a" figures are the nominal cases, while the "b" figures show the plots for half of the lox pump/thrust gain ($g_L/2$). Such variations are used to find the gain margin; e.g., by linear extrapolation we find that the 5 Hz range is approximately 5 db unstable for AS-502 while the same frequency range becomes 6 db stable for AS-504. The accuracy of the margin prediction can be increased by plotting new gain cases in an iterative fashion. Thus we can find margins with any degree of precision while the plots always indicate exactly whether the system is stable or unstable.

One may imagine a -1 point at the plot's origin but note that the loop gain is not a simple factor, merely one parameter or several dependent parameters which are buried in a loop-type transfer function.

Conclusions

Propulsion-generated oscillations had a history of occurrence up to the Saturn V vehicles in which an accumulator was successfully used for stabilizing pogo oscillations of the first flight stage. A particular problem, not experienced before the Saturn V series, was the multiple feedback of two essentially independent moving thrust forces and a large number of participating vehicle resonances.

The stability analysis shown appears very useful for complex systems or systems with matrix feedback. The concept of closed loop analysis is emphasized as a means to analyze stability with an inverted transfer function matrix. The pogo loop analysis of the Saturn V space vehicle demonstrated that a single Nyquist plot about the origin can advantageously be used to prove stability of a multivariable feedback system.

---

*The programing effort of Mr. W. F. Crumbley of MSFC's Computation Laboratory is gratefully acknowledged.

FIGURE 6a. SATURN V FIRST FLIGHT STAGE OF AS-502 MISSION AT 120 SEC FLIGHT TIME

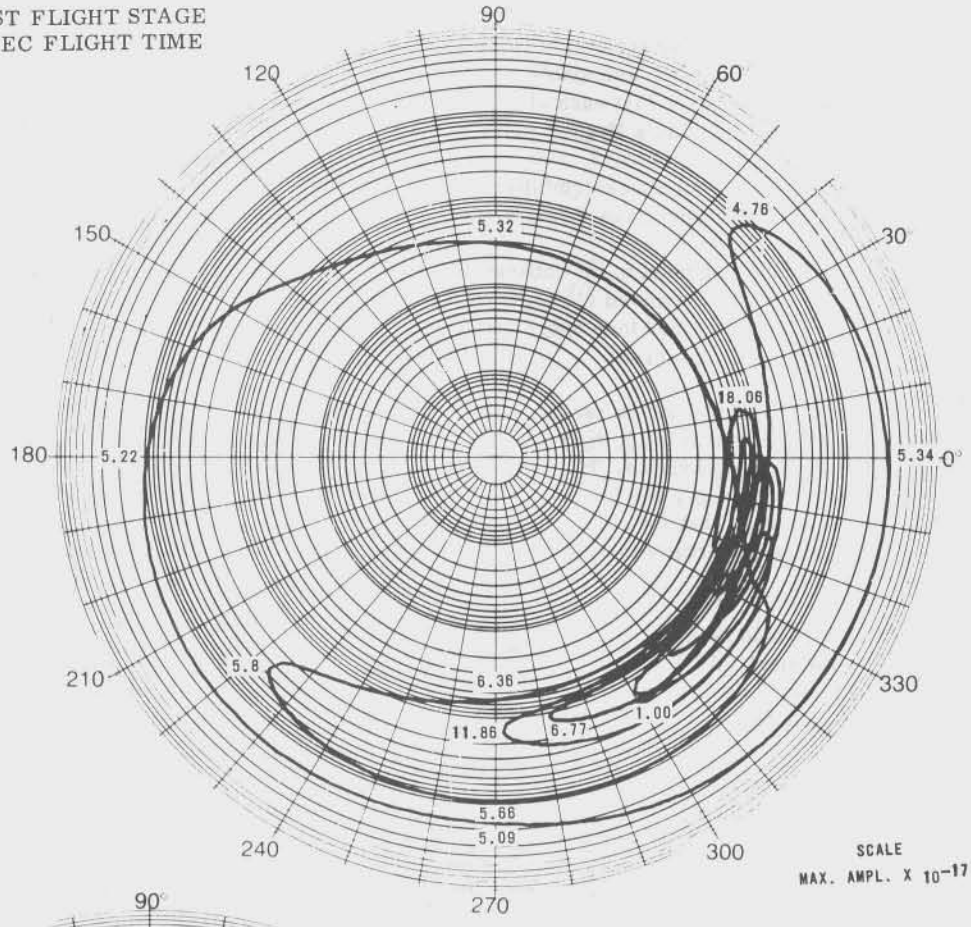

FIGURE 6b. SATURN V FIRST FLIGHT STAGE OF AS-502 MISSION WITH 1/2 OF LOX PUMP/THRUST GAIN

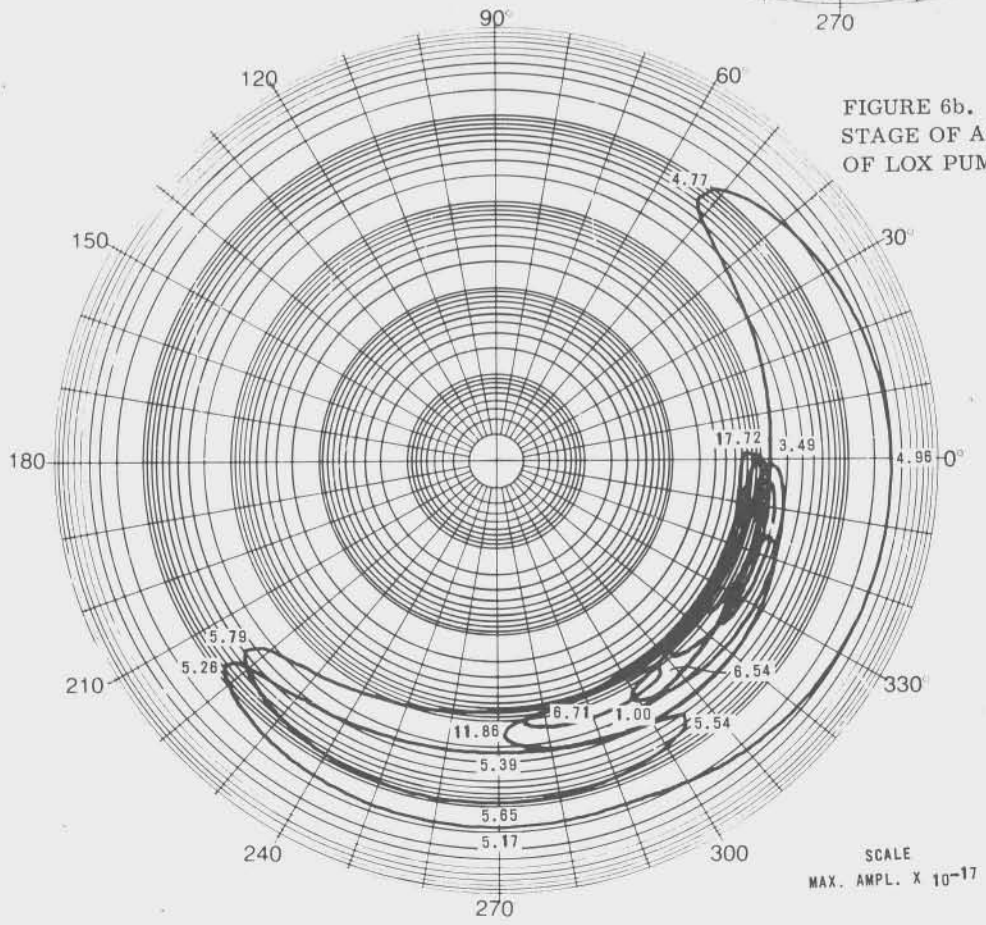

FIGURE 7a. SATURN V FIRST FLIGHT STAGE OF AS-504 MISSION AT 120 SEC FLIGHT TIME

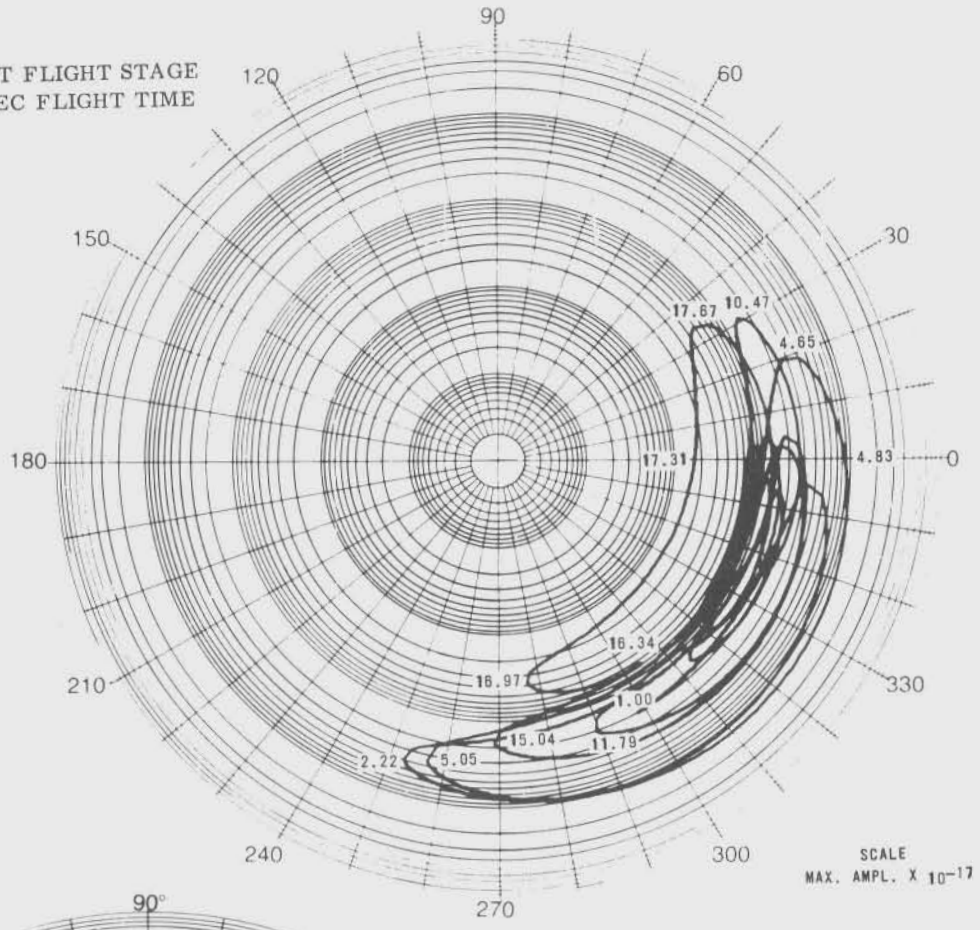

FIGURE 7b. SATURN V FIRST FLIGHT STAGE OF AS-504 MISSION WITH 1/2 OF LOX PUMP/THRUST GAIN

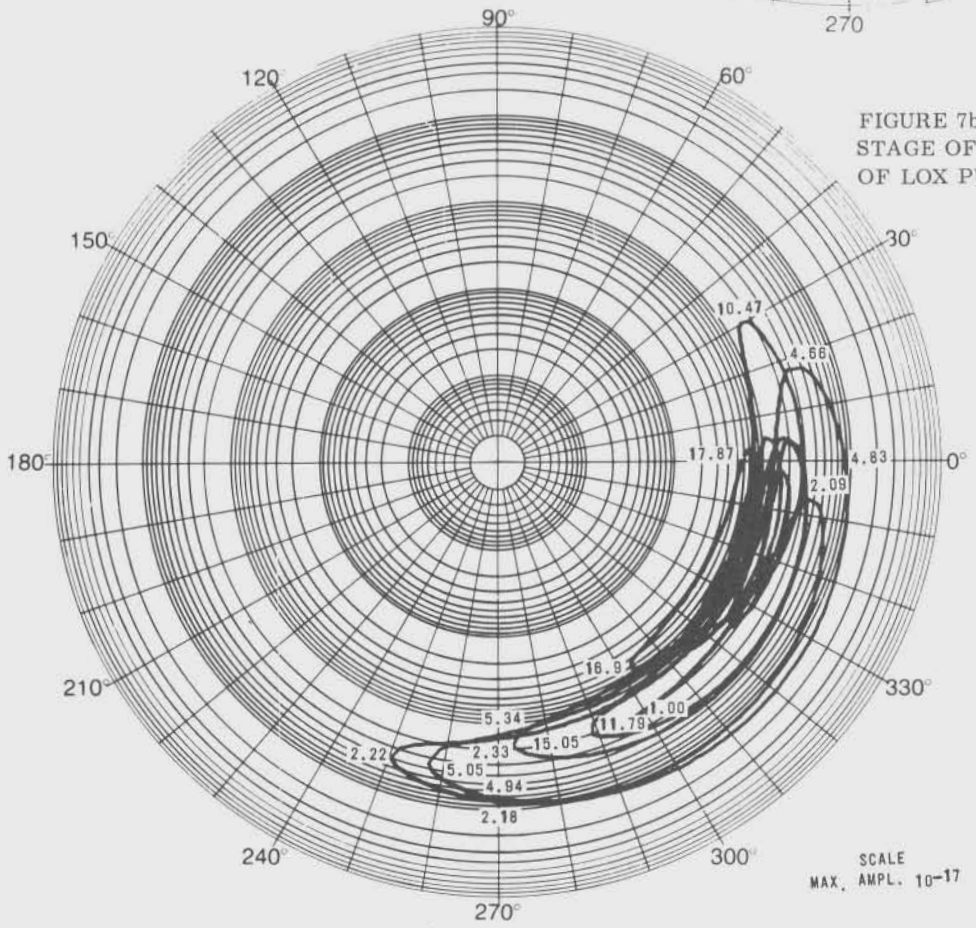

69-877

Nomenclature

A	4×4 pogo loop feedback matrix
adj A	4×4 adjoint of matrix A
B	2×4 matrix coupling disturbance forces
C	4×4 matrix relating interface forces to propellant forces, C_I for inboard engine, and C_O for outboard engine group
D	1×2 disturbance force row vector
D_I, D_O	disturbance force at inboard and outboard engine group, respectively
D_S	dashpot constant of simplified pogo model
E	thrust gain constant of simplified pogo model
f	disturbance force on simplified pogo model
F	vector of external forces on eigenvalue model
F_F	interface force on fuel feed line, F_{FI} for inboard, and F_{FO} for outboard
F_L	interface force on lox feed line, F_{LI} for inboard, and F_{LO} for outboard
F_s	total force of simplified pogo model
G	2×1 thrust gain matrix, G_I for inboard, and G_O for outboard
g_F, g_L	thrust gain for fuel and lox side, respectively
H	constant matrix of state vector equation
I	identity matrix
K	2×2 cavitation stiffness matrix, K_I for inboard, and K_O for outboard
K_e	stiffness matrix of eigenvalue model
K_F, K_L	cavitation stiffness on fuel pump inlet and lox pump inlet, respectively
K_N	2×2 cavitation stiffness matrix for eigenvalue model
K_s	cavitation stiffness on simplified pogo model
LOX	liquid oxygen oxidizer
M	mass matrix of eigenvalue model
m	structural mass of simplified pogo model
m_s	lox mass of simplified pogo model
m_i	generalized mass of eigenvalue model
P	1×2 propellant force variation vector
P_F	propellant force variation of fuel side, P_{FI} on inboard, and P_{FO} on outboard
P_L	propellant force variation on lox side, P_{LI} on inboard, and P_{LO} on outboard
P_s	propellant force variation in simplified model
Q	2×2 engine flow matrix
q_{FF}, q_{FL}	flow matrix element from fuel force to fuel flow and to lox flow, respectively
q_{LF}, q_{LL}	flow matrix element from lox force to fuel flow and to lox flow, respectively
s	Laplace operator
U	mode shape matrix or transformation matrix of eigenvalue model
T	thrust force variation on simplified pogo model
T_I, T_O	thrust force variation on inboard and outboard engine group, respectively
V_F, V_L	fuel and lox velocity, respectively
y	displacement vector in eigenvalue model
y_F	fuel displacement upstream of cavitation stiffness, y_{FI} for inboard, and y_{FO} for outboard
y_{F1}	fuel pump displacement; y_{L1} for lox
y_{F2}	fuel displacement downstream of cavitation stiffness; y_{L2} for lox

y_{F3} fuel displacement upstream of cavitation stiffness; y_{L3} for lox

y_I, y_O inboard and outboard engine displacement respectively

y_L lox displacement upstream of cavitation stiffness, y_{LI} for inboard, and y_{LO} for outboard

$\Delta Y_{FI}=Y_{FI}-Y_I$ inboard fuel mode vector difference

Y_{FI}, Y_{FO} fuel mode column vector upstream of inboard and outboard cavitation stiffness, respectively (one component per resonance)

$\Delta Y_{FO}=Y_{FO}-Y_O$ outboard fuel mode vector difference

Y_I, Y_O inboard and outboard engine mode column vector, respectively (one component per resonance)

$\Delta Y_{LI}=Y_{LI}-Y_I$ inboard lox mode vector difference

Y_{LI}, Y_{LO} lox mode column vector upstream of inboard and outboard stiffness, respectively (one component per resonance)

$\Delta Y_{LO}=Y_{LO}-Y_O$ outboard lox mode vector difference

z transformed displacement vector in eigenvalue model

Ω^{-1} diagonalized transfer function matrix of eigenvalue model

ω_i resonances of eigenvalue model in radians

ζ_i damping value of resonances ω_i

References

1. Bikle, F.: An investigation of longitudinal oscillation instability of the Saturn-V LOR vehicle. Interim Technical Summary Report, CR-65-43, Martin Marietta Corp., Denver, Colo. July 1965.

2. Davis, W. F., Keeton, D. L., and Lynch, T. E.: Thor longitudinal oscillation study. Report SM-45009, Douglas Missile and Space Systems Division, Santa Monica, Cal., March 1964.

3. Fashbauch, R. H., and Streeter, V. L.: Resonance in liquid rocket engine systems. Applied Mechanics Fluid Engineering Conference (American Society of Mechanical Engineers), Washington, D. C., June 7-9, 1965,

4. Rose, R. G., Staley, J. A., and Simson, A. K.: A study of system-coupled longitudinal instabilities in liquid rockets, part 1-analytical model. Report by General Dynamics/Convair, San Diego, Cal., September 1965.

5. Rubin S.: Longitudinal instability of liquid rocket due to propulsion feedback (Pogo). Journal of Spacecraft and Rockets, vol. 3, August 1966.

6. Worlund, A. L., Glasgow, V. L., Norman, D. E., and Hill, R. D.: The reduction of pogo effects by gas injection. AIAA Second Propulsion Joint Specialist Conference, Colorado Springs, Colo., June 13-17, 1966.

7. Goerner, E. E.: Lox prevalve to prevent pogo effect on Saturn 5. Space/Aeronautics, December 1968.

8. Rocketdyne, North American Inc.: Engine system transfer functions for support of S-V vehicle longitudinal stability (pogo) analysis program. Report R-6929, Canoga Park, Cal. March 8, 1967.

9. Dent, E. J.: Feedline analysis for inclusion in pogo stability programs. Memorandum C1-SRL-2-001-4, Brown Engineering Co., May 1966.

10. Bellman, R.: Introduction to matrix analysis. McGraw-Hill Book Co., Inc., New York, 1960, pp. 35,36.

11. Zadeh, L. A., and Desoer, C. A.: Linear System Theory. McGraw-Hill Book Co., Inc., 1963, pp. 311, 312.

12. Derusso, P. M., Roy, R. J., and Close, C. M.: State variables for engineers. John Wiley and Sons, Inc., 1965.

13. Chen, C. T.: Representation of linear time invariant composit systems. IEEE Transactions on Automatic Control, vol. AC-13, no. 3, June 1968, pp. 227-285.

14. Chen, C. T.: Stability of linear multivariable feedback systems. Proceedings of the IEEE, vol. 56, no. 5, May 1968.

15. Schwarz, H.: Mehrfachregelung, Grundlagen einer Systemtheorie. Springer Verlag, New York, 1967, pp. 244-251.

16. Nyquist, H.: Regeneration Theory. Bell System Technical Journal, vol. 11, 1932, pp. 126-147, republished by Bellman, R., and Kalaba, R: Mathematical trends in control theory. Dover Publication, Inc., New York, 1964.

17. Newton, G. C., Jr., Gould, L. A., and Kaiser, J. F.: Analytical design of linear feedback control. John Wiley and Sons, Inc., 1961, pp. 302-309.